Available online at www.sciencedirect.com

SciVerse ScienceDirect

Ceramics International 38 (2012) 2711–2718

CERAMICS INTERNATIONAL

www.elsevier.com/locate/ceramint

Effect of sodium dodecul sulfate on stability of gibbsite platelet stabilized emulsion foams

Wenjea J. Tseng *, Pei-Shan Wu

Department of Materials Science and Engineering, National Chung Hsing University, 250 Kuo Kuang Road, Taichung 402, Taiwan

Received 30 September 2011; received in revised form 15 November 2011; accepted 16 November 2011
Available online 25 November 2011

Abstract

Amphiphilic molecules of anionic sodium dodecul sulfate (SDS) were used to modify the hydrophobicity of cationic gibbsite platelets in aqueous foams prepared by mechanical frothing. Contact-angle (θ) measurements revealed that the originally hydrophilic particles with an apparent θ of $\sim 30^{\circ}$ become partially hydrophobic, $\theta > 50^{\circ}$, as the SDS concentration increased above $\sim$1 mM. Stable foams with up to 20 h duration were rendered with the preferential adsorption of the partially hydrophobized platelet particles (SDS $\geq$ 2.9 mM, solids concentration of 10 vol.%) at the water–air interface so that coalescence and disproportionation (i.e., Ostwald ripening) of the air-in-water (a/w) bubbles are suppressed. Macroporous alumina foams consisting of both open and closed pore structure, a mean cell diameter of about 300 μm, a sharp cell wall, and a relative porosity of 90% were produced by firing the dried gibbsite foams to 1500 °C in air atmosphere.

Keywords: Porous Foam; Gibbsite; Emulsion; Stabilization

1. Introduction

A recurrent interest on Pickering emulsions [1], i.e., stabilization of wet foams rendered by the presence of well-anchored particles at the dissimilar liquids or liquid–air interface first reported by Ramsden [2], is based upon the covering particles that provide an elastic and mechanically robust, and a functionally tailored shell texture vital to various emerging applications [3–5]. The presence of packing particles with a suitable wettability to reside preferentially at the interface is favored by the reduction of overall interface energy around the emulsion droplets [3]. This gives rise to a stable foam by hindering coalescence, drainage, and disproportionation (i.e., Ostwald ripening) of the bubbles over a long period of time typically longer than days or even months in comparison to merely minutes when only organic surfactants with long-chain carbon molecules in particular were used for the emulsification [6]. In view of the literature, macroporous alumina foams have been produced directly from the particle-stabilized mechanical frothing with a targeted usability in heterogeneous catalysis, separation, filtration, and refractory insulation [7–14]. Neirinck et al. [7] prepared alumina particles stabilized water-oil emulsions and obtained sintered macroporous alumina foams with a tailored pore size by using electrophoretic deposition and slip casting as the shaping method. Gonzenbach et al. [8,9] were the first to use short-chain fatty acids as amphiphiles with an aim that a suitable hydrophobization of the originally hydrophilic colloidal alumina surface can be prepared in aqueous water. The preferential attachment of the acid molecules on the particle surface was imparted through an electrostatic-driven adsorption, leading to productions of stabilized foams because of the existence of the partially hydrophobized colloidal particles. A suspension of high solids concentration could be used, which promotes a strong affinity for the particles to reside at the air–water interface as well as a formation of attractive particulate networks through percolation over the entire cellular foams. Similarly, Akartuna et al. [10] used short-chain propionic acid amphiphiles to modify the surface of alumina particles in water–oil liquids. The particle-stabilized emulsions were viscoelastic with an apparent yield stress. This finding allows production of the cellular alumina ceramics of complex shapes by use of existing plastic forming techniques such as injection molding and extrusion. Recently, the particle-stabilized

* Corresponding author. Tel.: +886 4 2287 0720; fax: +886 4 2285 7017.
E-mail address: wenjea@dragon.nchu.edu.tw (W.J. Tseng).

0272-8842/$36.00
doi:10.1016/j.ceramint.2011.11.039

wet foams have been extended to the preparation of various macroporous composites with tailored compositional distribution and pore morphology by modifying the wettability of the composite particles in liquids [11]. Formation of porous alumina–poly(vinylidene fluoride) composites was demonstrated. Alumina foams without the need of prolonged drying and sintering after the forming step have been developed by adding calcium aluminate cement into the surface-modified alumina suspensions so that the wet foams can be shaped and then self-set at room temperature [12,13]. In addition, macroporous alumina ceramics with aligned microporous walls were fabricated by Yoon et al. [14] through a unidirectional freezing of foamed alumina suspensions stabilized by adsorption of polyvinyl alcohol (PVA) polymers on the particle surface. The PVA serves as both a binder and an emulsifier.

While all the aforementioned wet-foam processes used high purity, spherical alumina particles as the starting material, this study intends to use gibbsite, $Al(OH)_3$, which is one of the important mineral forms of aluminum hydroxides, for the synthesis of alumina foams. The structure of gibbsite lacks proper bonding to keep the basic gibbsite layers together and therefore, leads to an easy cleavage of the layers by an applied shear stress. Well-dispersed platelets would in theory favor to reside and accumulate at the water–air interface with a plane orientation in line with the interface, creating ''armored'' foams with a mechanical barrier to the bubble coalescence and disproportionation [15]. A reduced particle concentration in suspensions is hence anticipated in order to render a stable foam because of the more efficient coverage of the platelets on the air-in-water (a/w) bubbles, leading to a macroporous alumina with a possibility of greater porosity and lighter weight after firing. In this study, an anionic surfactant of sodium dodecul sulfate (SDS) was used to modify the hydrophobicity of the cationic gibbsite platelets in aqueous wet foams through the electrostatic adsorption. In addition, a simple, static sessile drop contact-angle goniometer was used as a semiquantitative measure for evaluating the *apparent* wettability of the gibbsite particles with the various degrees of surface modifications, despite advances in determining the three-phase contact angle of *single* nanoparticle in liquids have been made available recently [16].

2. Experimental procedure

2.1. Materials

The gibbsite particles were kindly provided by Prof. Fu-Su Yen at the National Cheng Kung University (Taiwan). Reagent-grade sodium dodecul sulfate (SDS, $NaC_{12}H_{25}SO_4$, 99%, Aldrich, Japan), 1-dodecanol ($CH_3(CH_2)_{11}OH$, 98.6%, Tedia, USA), hydrochloric acid (HCl, 37%, Aldrich, Germany), and ammonia (NH_4OH, 28%, Aldrich, Germany) were all used without any treatment. De-ionized water (18.2 Ω cm) was prepared from Millipore Super-Q Plus (USA).

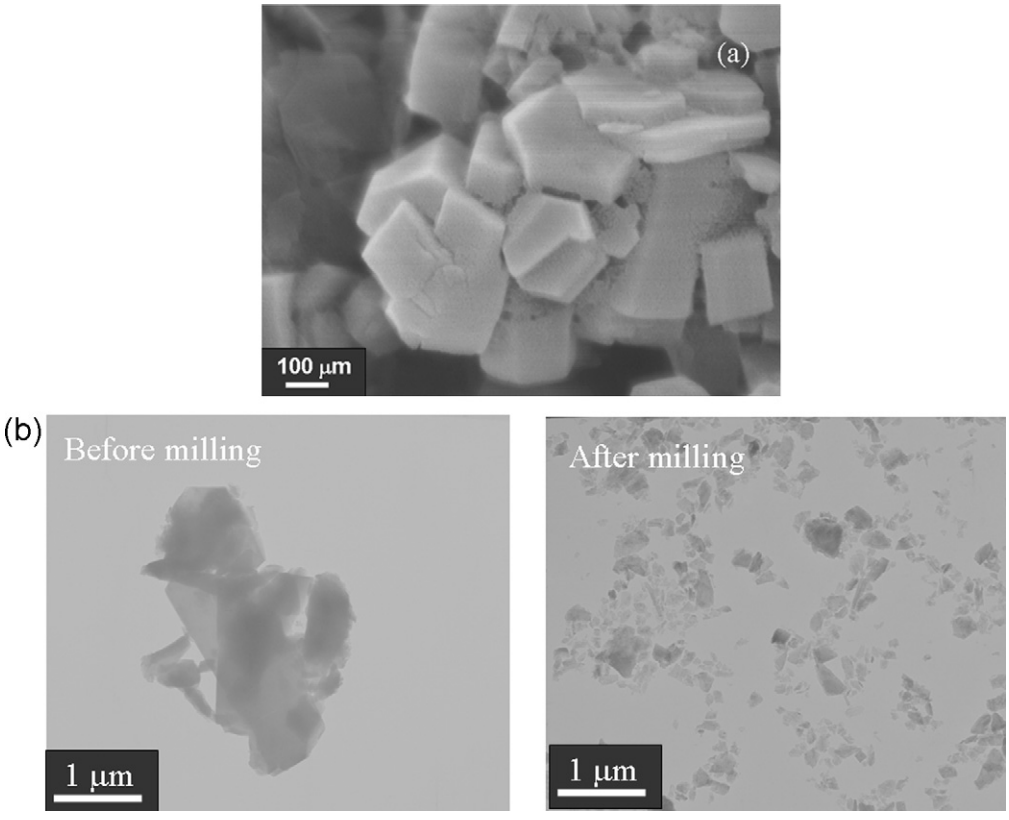

Fig. 1. (a) Particle morphology of the as-received gibbsite particles. (b) The TEM photos of the as-received and ball-milled gibbsite particles.

2.2. Foam preparation and stability observation

The as-received gibbsite particles were mixed with D.I. water, SDS, and 1-dodecanol in a fixed solids concentration of 10 vol.%. The SDS concentration varied from zero to 10.4 mM. The 1-dodecanol concentration was held at 16 mM while the suspension pH was kept at 2.5 ± 0.1 by addition of HCl solution (2 M). The powdered suspensions were ball-milled in polyethylene bottles by using high-purity alumina balls as the grinding medium for 20 h. Some of the wet foams prepared after the milling process were removed from the bottles and placed in a petri dish. The dish was then covered with a glass slide and sealed by using silicon grease at the interface ready for the optical measurement by placing a digital camera vertically above the glass-covered dish. The evolution of bubbles size with time was recorded continuously, and the fractional frequency for the bubbles over various average diameters (e.g., an average of 100 μm represents bubble diameters over a range from 50 to 149 μm) was plotted in histogram. Over 200 bubbles were counted for each sample. The remaining wet foams after milling were placed in molds of different geometries, dried in an oven at 75 °C for 24 h, and were then sintered to 1500 °C with 2 h isothermal holding in air atmosphere.

2.3. Characterization

The as-received gibbsite particles were examined by thermal gravimetric and differential thermal analyses (Diamond TG/DTA 6300, Perkin Elmer, USA) at a heating rate of 10 °C min^{-1} from ambient to 1000 °C in flowing air atmosphere to monitor the weight loss and thermal behavior of the particles. Crystalline structure of the as-received and calcined gibbsite particles was observed by X-ray diffractometry (MXP-III, Mac Science, Japan) using Cu Kα radiation (λ = 1.5406 Å) at a scanning speed of 2° min^{-1} from incident angles of 10° to 90°. Field-emission scanning electron microscopy (FE-SEM, JSM-6700F, JEOL, Japan) and transmission electron microscopy (TEM, JEM-2010, JEOL, Japan), operated at 200 kV acceleration voltage, were used for the microstructural examination. For the determination of zeta potential (Zetasizer NS, Malvern, UK) of the gibbsite particles, the ball-milled particles were mixed with D.I. water to form uniform dispersions via an ultrasonic homogenizer (Sonicator 3000, Misonix, USA) operated at 3 W in a circulating water bath kept at 25 °C. The solids loading used was of a dilute concentration (0.05 wt.%), while the suspension pH was adjusted with HCl (2 M) and NH_4OH (1 M). For the determination of the *apparent* contact angle, the dried particles (75 °C for 24 h) with various degrees of SDS modification were first pressed into discs (diameter of 13 mm) by a compression pressure sufficient to make the discs reach a relative density of $55 \pm 1\%$ of the theoretical. Typical compaction pressure ranged from 40 to 45 MPa. A sessile drop-shape analyzer (FTA 2000, First Ten Angstroms Inc., USA) was then used for the contact-angle measurement which dispenses water drops from a syringe pointed vertically down onto the surface-smooth discs at 25 °C and captures the water profile on the samples by an optical system. As the water drop first contacts the porous samples, the drop spreads on the surface and begins to permeate into the interstices of the packing particles. The permeation would cease as the water content in the powder compacts saturates, indicating a sufficient occupation of water in the packing interstices around the droplet site. This contact angle made by the intersection of the liquid–solid and liquid–air interfaces was then measured from the static shape of the drop through a goniometer. An average of at least five measurements was carried out for each batch of the gibbsite particles with the different SDS modifications. This measurement enables a direct comparison of the *apparent* contact angles from the powdered gibbsite compacts with various degrees of hydrophobicity. Mercury porosimetry (Autopore 9520, Micromeritics, USA) was used to measure the pore size and pore volume of the sintered alumina foams prepared from plates with a dimension of ca. 0.5 cm × 0.5 cm × 1.0 cm. The testing samples were first evacuated to remove air and moisture before applying various levels of pressure to the samples immersed in mercury. A maximum pressure of 414 MPa was used for the measurement.

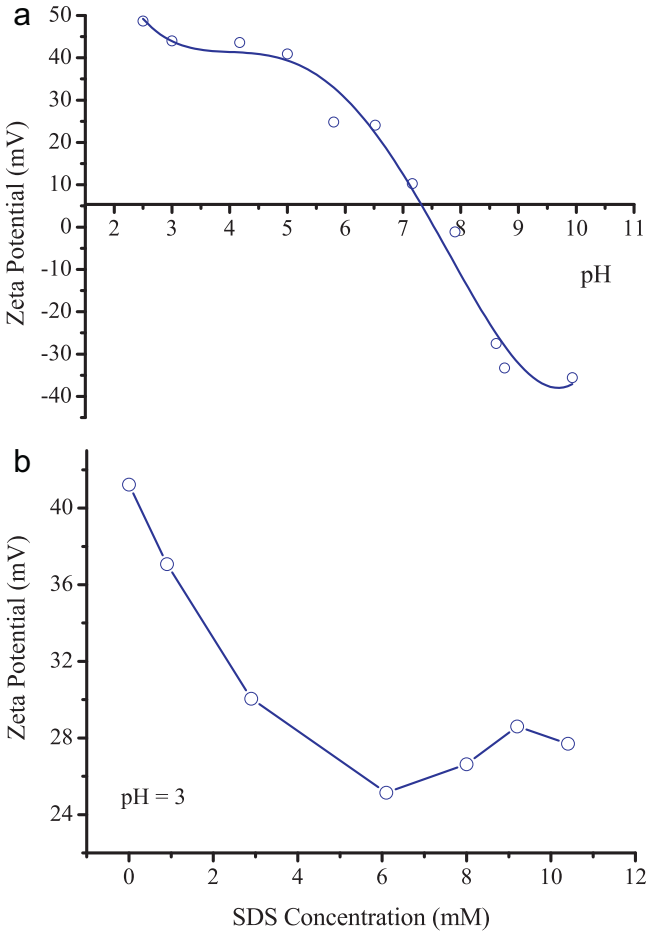

Fig. 2. (a) Zeta potential of the gibbsite particles at various pHs. (b) The change of zeta potential of the gibbsite-filled aqueous suspension with SDS concentration at a constant pH of 3.

3. Results and discussion

3.1. Morphology, structure, and surface potential of the gibbsite particles

Fig. 1 shows the morphology of gibbsite particles. Stacked, prismatic sheets of aluminum hydroxide form the basic structure of the as-received particles in Fig. 1a. The platelet diameter spans over a wide range from ~100 nm to 20 μm, and with a sheet thickness of ~30 nm to 1 μm. Fig. 1b shows TEM microstructure of the gibbsite particles with and without the ball milling. The milled particles show a substantially reduced platelet diameter (<500 nm) and appear to be less agglomerated. Upon subjected to heating, the gibbsite particles tend to release free, adsorbed water at temperatures under 250 °C, and begin to decompose to boehmite (AlOOH) by loosing the crystallization water with a substantial weight loss (~32%) when temperature was raised further [17,18]. A pronounced endothermic peak is found at 260 °C from the thermal analyses. XRD verifies that the particles were indeed transformed from gibbsite to boehmite (JCPDS 83-2384) at 300 °C. The particles then change from boehmite to γ-Al_2O_3 (JCPDS 10-425) as temperature was further raised to 600 °C, confirmed also by XRD.

The zeta (ζ) potential determined from the electrophoretic mobility is shown in Fig. 2a. The isoelectric point (IEP) is determined at pH ~ 7.4, at which pH value the particles in suspension would agglomerate most rapidly because of the absence of interparticle repulsion to overcome the van der Waals attraction. At pH values lower than the IEP, the particles bear a positive surface charge that can attract the anionic SDS molecules in liquid, resulting in a partially hydrophobic particle surface because of the coverage of the surfactant molecules with a non-polar tail that replaces the initially hydrophilic gibbsite surface. In addition, an acidic pH sufficiently away

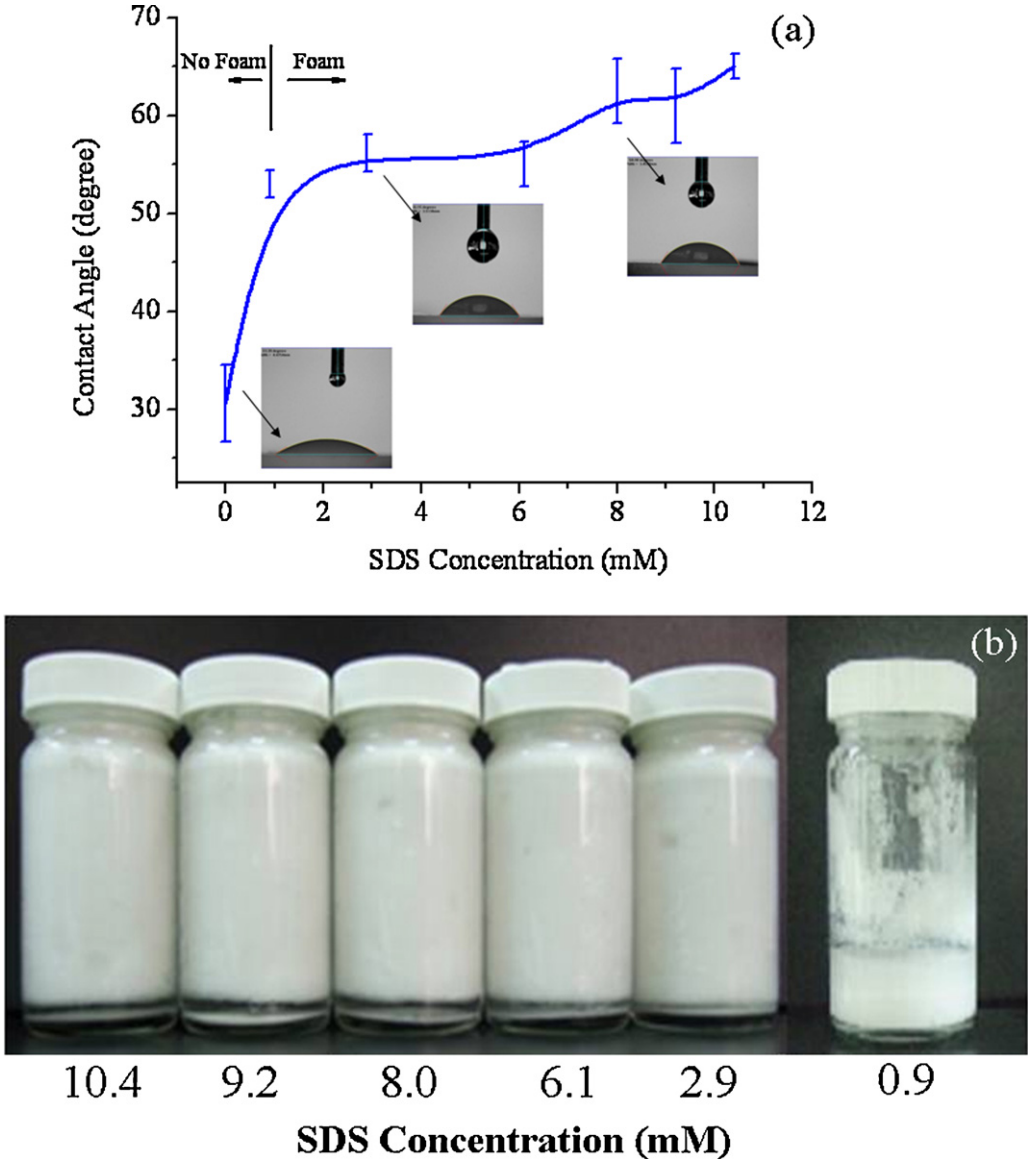

Fig. 3. (a) Contact angle vs. SDS concentration of the gibbsite-filled aqueous suspensions. The solids loading was held at 10 vol.%. (b) Vials of the gibbsite foams with various SDS concentrations after being placed without disturbance for 20 h.

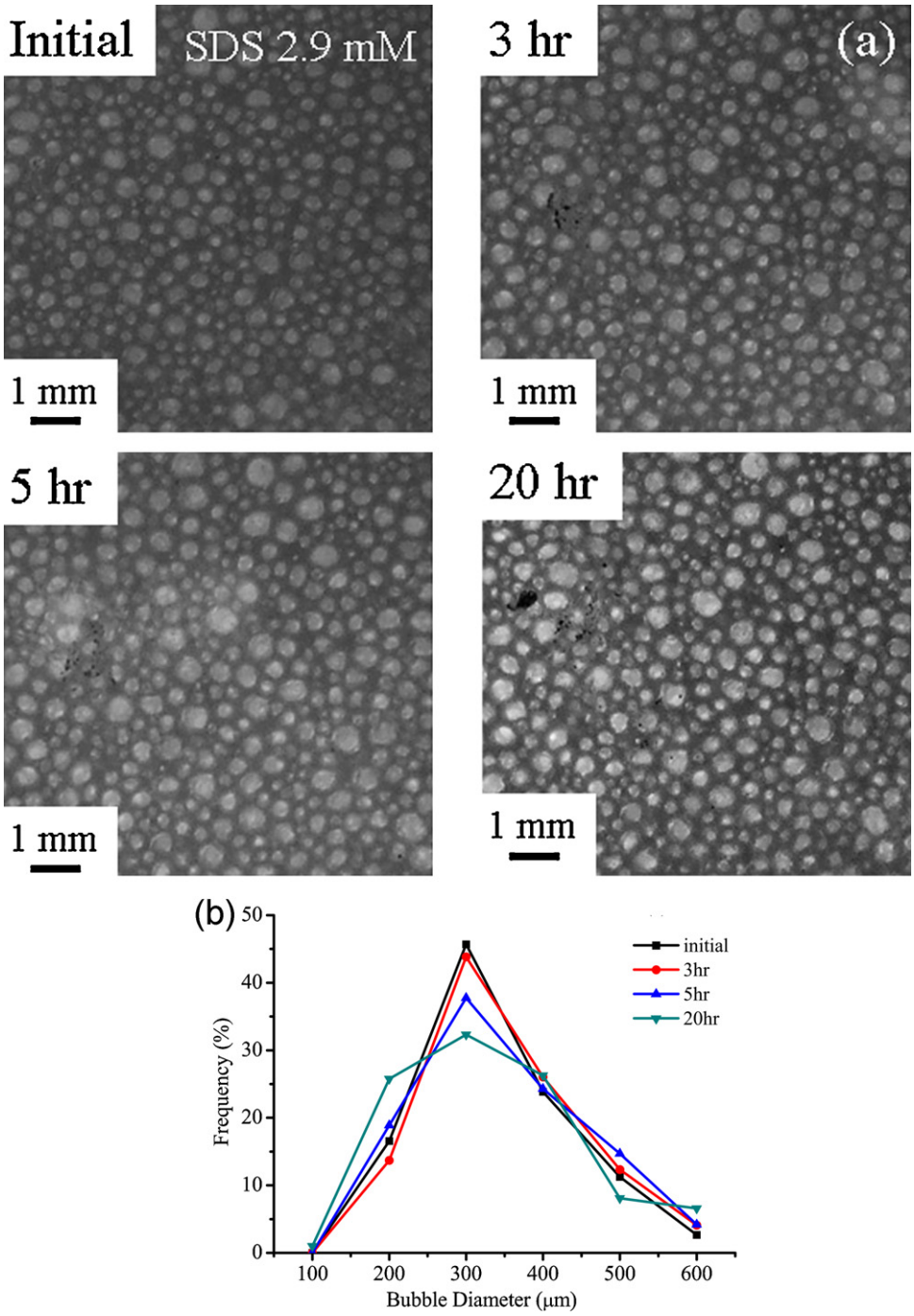

Fig. 4. (a) Digital photographs of the gibbsite-stabilized foams with time. The SDS concentration was 2.9 mM. (b) Histogram of the bubble-size evolution of (a).

from the IEP would facilitate the stabilization of platelet particles in water because of the existence of an electrostatic repulsion when particles are brought in close proximity. In this regard, a pH = 3 was selected for the particulate suspensions at which the ζ potential saturates at a reasonable high value ($\zeta = 43$ mV). In Fig. 2b, the ζ potential is found to decrease rapidly from 43 to 25 mV as the SDS concentration increases from zero to 6 mM while the suspension pH was held at pH = 3, revealing that the anionic surfactants were adsorbed preferentially on the cationic gibbsite surface. The ζ potential then increases as the SDS concentration further increased. The reversion occurs at a SDS concentration close to the critical micelle concentration (CMC) of the SDS, i.e., 8.2 mM in pure water at 25 °C. One might suspect that the adsorption of SDS molecules on the platelet surface may in fact be reversible so that some of the already adsorbed molecules would desorb from the surface and attach one another into micelles in the water liquid and vice versa. As the SDS concentration exceeds its CMC, the formation of micelle is therefore favored than that of the adsorption on gibbsite surface, leading to the reverse increase of ζ potentials.

3.2. SDS concentration on foam stability

The *apparent* contact angles measured from the drop-shape method are shown in Fig. 3a for the surface-modified gibbsite particles with various SDS concentrations. Typical drop-shape photos are representatively shown for comparison reasons. Without the SDS, the gibbsite surface is hydrophilic with an average $\theta \sim 30^{\circ}$. The surface quickly becomes partially hydrophobic when modified with the SDS, and appears to reach a plateau with an average $\theta > 50^{\circ}$ as the SDS concentration increased above ~1 mM. This together with the observation of Fig. 2b indicates that the preferential adsorption of the anionic SDS molecules on the cationic gibbsite surface has given rise to a more hydrophobic surface by

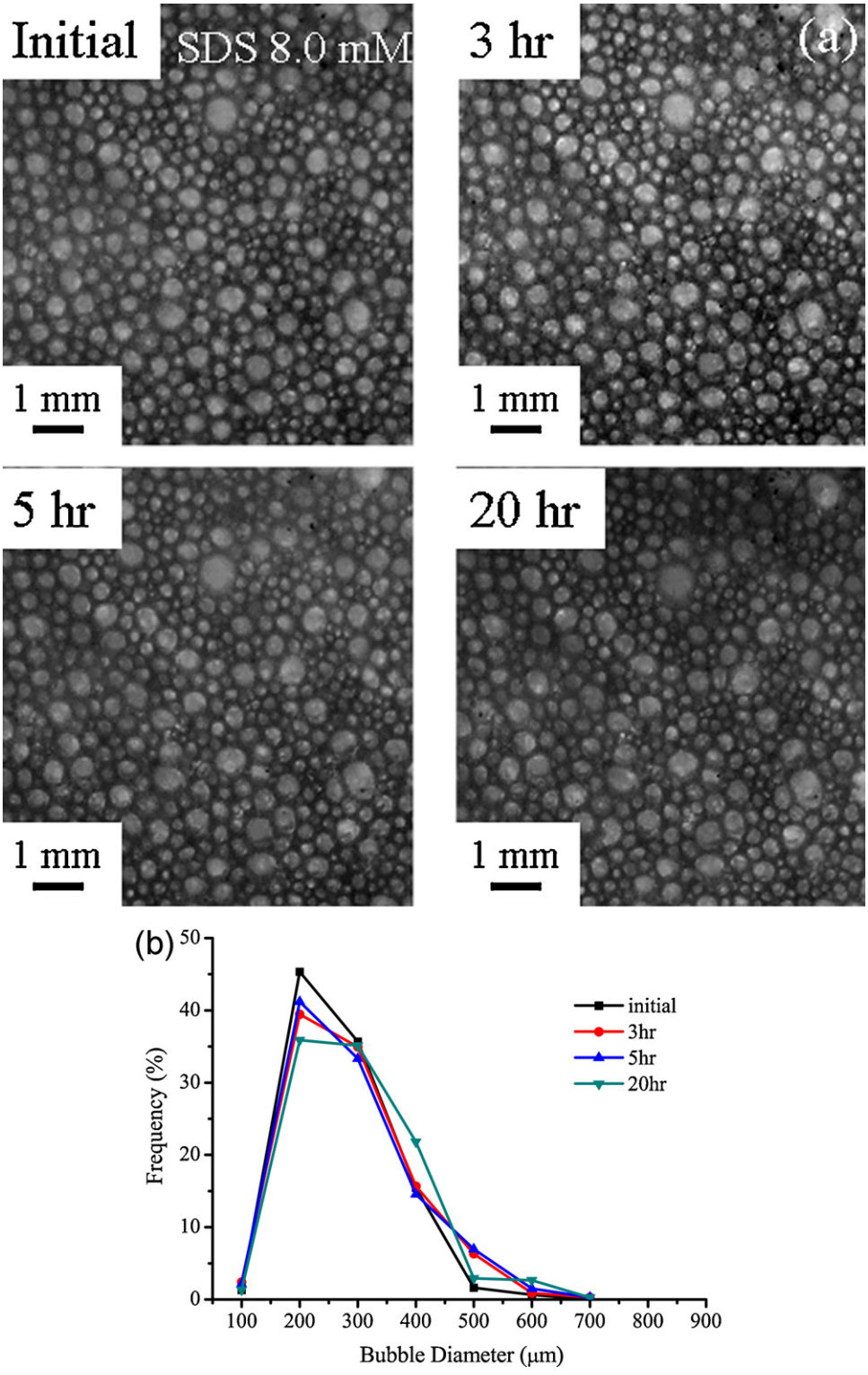

Fig. 5. (a) Digital photographs of the gibbsite-stabilized foams with time. The SDS concentration was 8.0 mM. (b) Histogram of the bubble-size evolution (a).

exposing the non-polar end of the molecules toward the polar liquid in replacement of the originally hydrophilic gibbsite surface. The saturation of the apparent contact angle suggests that a monolayer adsorption of the SDS molecules resulted before the SDS concentration reached its CMC (< 8 mM). The SDS molecules then form micelles spontaneously when the concentration exceeds the CMC level. The free micelles in liquid would deposit on the surface of the surface-modified platelets when subjected to the drying process, and remain on the platelet surface and/or the interstices between the platelets after the molding compression to form discs for the contact angle measurement. One would expect that the contact angle measured would actually decrease because of the existence of micelles; nonetheless, the opposite is found and the contact angle indeed appears to increase with the micelle fraction. Since the compaction pressure (>40 MPa) involved in the disc-forming process was well above the strength of the micelle, most of the micelles were expected to collapse on the platelet surface that can be regarded essentially as the multiple deposition layers, leading to a densely packed SDS layers on the particle surface so that the hydrophobicity increased. This argument agrees well with the observation of an increased plateau as the SDS concentration exceeds its CMC in Fig. 3a. In line with the contact angle results, Fig. 3b shows that stable foams were formed after 20 h duration with the adsorption of the partially hydrophobized platelet particles when the SDS concentration was greater than 2.9 mM. This indicates that coalescence and disproportionation (i.e., Ostwald ripening) of the a/w bubbles were suppressed significantly.

Evolution of the bubble-size distribution with time has been evaluated by the digitized photos placed vertically on the bubbles-filled dishes. As shown representatively in Fig. 4a, the a/w bubbles present a wide size distribution, i.e., the average size ranges from 100 to 600 μm from the platelet suspensions with the SDS concentration of 2.9 mM. As time progressed, some bubbles appear to grow at the expense of neighboring small ones. Fig. 4b shows a substantially broader size distribution as the duration time exceeded 3 h while the average bubble size remained at 300 μm, i.e., 250 to 350 μm, with a reduced fractional frequency. In comparison, Fig. 5a shows that the a/w bubbles present a size distribution with a smaller average size (ca. 200–300 μm) and a longer ''tail'' toward the greater size (≥400 μm) for the platelet suspensions with the SDS concentration of 8.0 mM. The foam morphology remains relatively stable. In Fig. 5b, reduction in the fractional frequency at the prime bubble size occurs but with a lesser degree of significance for the same duration of 20 h. Note that a similar finding resulted for the foams with the SDS concentration greater than 8.0 mM. This is hence in good agreement with the contact angle results; to which, the wettability of the gibbsite particles in water can be tailored to a suitable hydrophobicity by the SDS adsorption so that a relatively stable foam with a reduced drainage, coalescence and disproportionation can be rendered. However, the average bubble size with 20 h duration appears not being altered significantly, i.e., from ca. 350 to 275 μm for the suspensions with the SDS concentration of 2.9 and 10.4 mM, respectively, within the resolution of the digitized photos used. This reveals that the SDS concentration did not vary the bubble diameter. Other process variables, such as mechanical agitation and temperature involved in the mechanical frothing process may be critically important to the determination of bubble size.

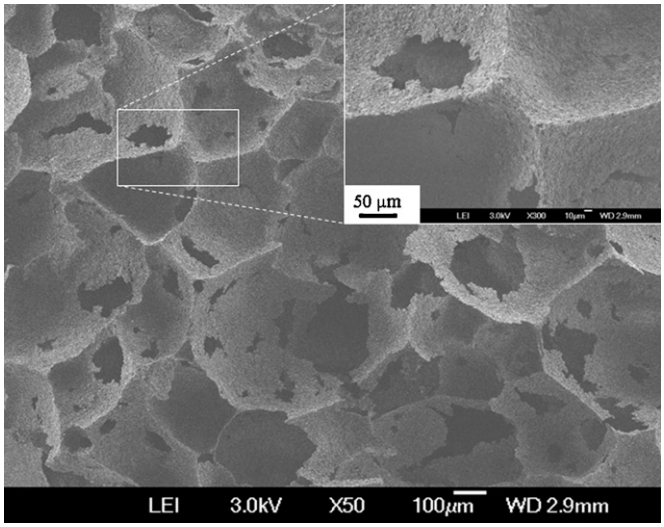

Fig. 6. Microstructure of the alumina foams fired at 1500 °C in ambient air atmosphere. The inset shows an enlarged section of the micrograph.

3.3. Cellular foam structure and porosity

Fig. 6 shows the microstructure of the alumina foams fired at 1500 °C. Note that the SDS concentration was held at 8 mM for the foam preparation. The foams are macroporous with a cell diameter ranging from ca. 200 to 500 μm and a sharp cell wall. The platelet concentration used in the suspension (10 vol.%) was apparently not sufficient to provide a full coverage of all the bubble interfaces produced, creating open channels between neighboring cells. This finding suggests that the cell structure can be tailored from partly open cell to fully close cells by tuning the solids loading in the suspension process. In addition, the inset shows some particles on the cells remain a sheet form, resulting in the sharp cell wall. From the mercury porosimetry, a low bulk density of 0.41 g cm^{-3} (equivalent to a relative density of 10.2% at a mercury pressure of 3.2 kPa) and an apparent density of 1.80 g cm^{-3} (equivalent to a relative apparent density of 45.2% at a mercury pressure of 414 MPa) resulted. The fired foams, therefore, consisted of both closed (54.8%) and open pores (35%). The average pore diameter connecting the open cells of the cellular foams is merely 2.6 μm from the mercury porosimetry, which is dramatically different from the microstructure observation shown in Fig. 6. This reveals that inhomogeneous pore channels exist in the cellular foams, so that the mercury intrusion needs to pass through small pore openings (i.e., channels formed by the interstices between bubbles) before entering into large cells.

4. Conclusion

Amphiphilic SDS molecules have been preferentially adsorbed on surface of cationic gibbsite platelets in aqueous water so that the hydrophobicity of the gibbsite particles can be tailored to prepare stable foams by mechanical frothing. The foam stability is confirmed by contact-angle measurements, in which θ varied from the originally hydrophilic particles ($\theta \sim 30^{\circ}$) to partially hydrophobic ($\theta > 50^{\circ}$) as the SDS concentration increased above $\sim$1 mM. In addition, the foams are also examined by a direct observation of cell size with time; to which, stability up to 20 h duration was rendered for the platelet-armed foams with the preferential SDS adsorption. Macroporous alumina foams consist of both open and closed pore structure in a volumetric ratio of 1:1.6, a mean cell diameter of about 300 μm, a sharp cell wall, and a relative porosity of ca. 90% after firing the dried gibbsite foams to 1500 °C in air atmosphere. The pore channels are found highly inhomogeneous; therefore, intrusion liquids need to pass through small opening channels before entering into the void cells.

Acknowledgments

We gratefully acknowledge Prof. Fu-Su Yen at the Department of Resources Engineering of the National Cheng Kung University for providing the gibbsite particles. Financial support from the National Science Council (Taiwan, ROC) under contract no. NSC 98-2221-E-005-031-MY3 is also gratefully acknowledged.

References

[1] S.U. Pickering, Emulsions, J. Chem. Soc. 91 (1907) 2001–2021.
[2] W. Ramsden, Separation of solids in the surface-layers of solutions and 'suspensions' (Observations on surface-membranes, bubbles, emulsions, and mechanical coagulation). Preliminary account, Proc. R. Soc. Lond. 72 (1903) 156–164.
[3] O.D. Velev, K. Furusawa, K. Nagayama, Assembly of latex particles by using emulsion droplets as templates. 1. Microstructured hollow spheres, Langmuir 12 (1996) 2374–2384.
[4] A.D. Dinsmore, M.F. Hsu, M.G. Nikolaides, M. Marquez, A.R. Bausch, D.A. Weitz, Colloidosomes: selectively permeable capsules composed of colloidal particles, Science 292 (2002) 1006–1009.
[5] B.P. Binks, Macroporous silica from solid-stabilized emulsion templates, Adv. Mater. 14 (2002) 1824–1827.
[6] A.R. Studart, U.T. Gonzenbach, E. Tervoort, L.J. Gauckler, Processing routes to macroporous ceramics: a review, J. Am. Ceram. Soc. 89 (2006) 1771–1789.
[7] B. Neirinck, J. Fransaer, O. Van der Biest, J. Vleugels, Production of porous materials through consolidation of Pickering emulsions, Adv. Eng. Mater. 9 (2007) 57–59.
[8] U.T. Gonzenbach, A.R. Studart, E. Tervoort, L.J. Gauckler, Ultrastable particle-stabilized foams, Angew. Chem. Int. Ed. 45 (2006) 3526–3530.
[9] U.T. Gonzenbach, A.R. Studart, E. Tervoort, L.J. Gauckler, Macroporous ceramics from particle-stabilized wet foams, J. Am. Ceram. Soc. 90 (2007) 16–22.
[10] I. Akartuna, A.R. Studart, E. Tervoort, L.J. Gauckler, Macroporous ceramics from particle-stabilized emulsions, Adv. Mater. 20 (2008) 4714–4718.
[11] J.C.H. Wong, E. Tervoort, S. Busato, L.J. Gauckler, P. Ermanni, Controlling phase distributions in macroporous composite materials through particle-stabilized foams, Langmuir 27 (2011) 3254–3260.
[12] F. Krauss Juillerat, U.T. Gonzenbach, A.R. Studart, L.J. Gauckler, Self-setting particle-stabilized foams with hierarchical pore structures, Mater. Lett. 64 (2010) 1468–1470.
[13] F. Krauss Juillerat, U.T. Gonzenbach, P. Elser, A.R. Studart, L.J. Gauckler, Microstructural control of self-setting particle-stabilized ceramic foams, J. Am. Ceram. Soc. 94 (2011) 77–83.
[14] H.J. Yoon, U.C. Kim, J.H. Kim, Y.H. Koh, W.Y. Choi, H.E. Kim, Macroporous alumina ceramics with aligned microporous walls by unidirectionally freezing foamed aqueous ceramic suspensions, J. Am. Ceram. Soc. 94 (2010) 1580–1582.
[15] N.P. Ashby, B.P. Binks, Pickering emulsions stabilised by laponite clay particles, Phys. Chem. Chem. Phys. 2 (2000) 5640–5646.
[16] L. Isa, F. Lucas, R. Wepf, E. Reimhult, Measuring single-nanoparticle wetting properties by freeze-fracture shadow-casting cryo-scanning electron microscopy, Nat. Commun. 2 (2011) 1–9.
[17] X. Yang, Z. Sun, D. Wang, W. Forsling, Surface acid–base properties and hydration/dehydration mechanisms of aluminum (hydr)oxides, J. Colloid Interface Sci. 308 (2007) 395–404.
[18] L.-T. Cheng, M.-Y. Tsai, W.J. Tseng, H.-I. Hsiang, F.-S. Yen, Boehmite coating on θ-Al_2O_3 particles via a sol gel route, Ceram. Int. 34 (2008) 337–343.